Physics – Uspekhi **67** (11) 1119 – 1128 (2024)

REVIEWS OF TOPICAL PROBLEMS

PACS numbers: **06.20. – f,** 37.10.De, 37.10.Jk

55th ANNIVERSARY OF THE INSTITUTE OF SPECTROSCOPY OF THE RUSSIAN ACADEMY OF SCIENCES (ISAN)

Laser cooling of thulium atoms to ground vibrational state in an optical lattice

D I Provorchenko, D O Tregubov, A A Golovizin, N N Kolachevsky

DOI: https://doi.org/10.3367/UFNe.2024.05.039678

Contents

Abstract. The method of laser cooling of atoms, first implemented in the early 1980s at the Institute of Spectroscopy of the Russian Academy of Sciences (ISAN), turned out to be an exceptionally powerful tool that provided revolutionary breakthroughs in such areas as quantum sensorics, the physics of Bose–Einstein and Fermi-condensates, quantum informatics, and many others. It was precisely due to the laser cooling method that atomic fountains — the most accurate microwave clocks — made their appearance, and impetus was lent to the area of optical frequency standards, which today have surpassed the relative error of 10^{-18}. In this review, dedicated to the 55th anniversary of the founding of ISAN, we will present some modern methods and experimental results aimed at the development of optical clocks on thulium atoms. In addition to the review part, the paper demonstrates a new experimental protocol for the preparation of thulium atoms using sideband cooling of the spectrally narrow 506.2-nm transition. Ensembles of atoms in the initial states of clock transitions in the ground vibrational sublevel of the optical lattice have been attained.

Keywords: laser cooling, thulium, optical frequency standards, spectroscopy, sideband cooling, optical lattices

D I Provorchenko [(1, a)], **D O Tregubov** [(1, b)], **A A Golovizin** [(1, c)], **N N Kolachevsky** [(1, 2, d)]
[(1)] Lebedev Physical Institute, Russian Academy of Sciences, Leninskii prosp. 53, 119991 Moscow, Russian Federation
[(2)] Russian Quantum Center, Innovation Center Skolkovo, Bol'shoi bul'var 30, srt. 1, 121205 Moscow, Russian Federation
E-mail: [(a)] provorchenko.di@phystech.edu.ru, [(b)] treg.dim@gmail.com, [(c)] artem.golovizin@gmail.com, [(d)] kolachevsky@lebedev.ru

Received 12 April 2024, revised 14 May 2024
Uspekhi Fizicheskikh Nauk **194** (11) 1185 – 1195 (2024)
Translated by E N Ragozin

1. Introduction

The discovery of the principle of laser-maser generation of electromagnetic radiation by N G Basov and A M Prokhorov in 1955 [1] led to the rapid development of laser physics: scientists around the world worked on the search for and study of new active media, cavity and pumping schemes, as well as the properties of laser radiation. However, by the early 1970s, lasers began to transform from an actual object of research into a tool that can be used to explore new horizons, in view of such properties of laser radiation as spectral purity, directionality, and high power density. One of the lines of research was laser spectroscopy, which makes it possible to precisely address individual transitions in atoms.

It is possible to list a number of key names with which we today associate pioneering ideas regarding the use of laser radiation in laser spectroscopy problems. First of all, it is N G Basov himself, as well as his closest colleague and student V S Letokhov [2], who proposed using laser radiation in optical frequency standards. Among the Russian luminaries of this area, we should also include V P Chebotaev, who formulated a number of key ideas on laser spectroscopy [3] and founded the Institute of Laser Physics of the Siberian Branch of the Russian Academy of Sciences. Their names deservedly enjoy the deepest respect throughout the world.

In 1968, the research by V S Letokhov's group was separated into an independent group and the Institute of Spectroscopy of the Russian Academy of Sciences (ISAN) was set up. And almost immediately, the research of this small but extremely successful and productive team reached the forefront. The idea of laser deceleration of atoms was in the air at that time: the mechanical effect of light on atoms had long been known, starting with the early work by P N Lebedev on the study of light pressure on gases [4]. Unfortunately, this work did not receive wide recognition, which is analyzed in Ref. [5]. The experiments by the German physicist Frisch [6] on the deflection of a sodium beam by

radiation from a resonant lamp, which were performed 23 years after Lebedev's work, are better known in the scientific community.

The advent of narrow-band laser sources, whose radiation frequency is tuned close to a strong atomic resonance transition, opened up completely new possibilities for controlling the state of motion. The idea of laser cooling was formulated by Hänsch and Schawlow [7] and independently by Wineland and Dehmelt [8] in 1975. All of these scientists were awarded the Nobel Prize in Physics for various achievements. Despite the fact that they were theoretical studies, the path to practical implementation was 'illuminated,' although a lot of theoretical and experimental questions remained.

And so, in 1981, harnessing the idea of chirping laser pulses to overcome the Doppler effect, a group of scientists from ISAN demonstrated for the first time laser deceleration of a beam of sodium atoms [9]. A little earlier, laser cooling of ions held in traps was reported [10]. It was precisely from the early 1980s that the era of laser cooling of atoms began, which continues triumphantly to this day, advancing both in fundamental and applied areas. A number of Nobel Prizes in subsequent years have been based on these principles; however, by a sad coincidence, there is not a single name of a Russian scientist among them. And, despite this, on its 55th anniversary, ISAN continues to occupy a world-leading position in this field, successfully implementing a number of bright and interesting ideas under the leadership of V I Balykin, one of the originators of the laser cooling circle.

Letokhov and Minogin showed in [11] that Doppler cooling has a lower temperature limit $T_{\mathrm{D}} = \hbar\Gamma/(2k_{\mathrm{B}})$, which includes the Boltzmann constant k_{B} and the spectral width of the excited level Γ. For typical electric dipole transitions $\Gamma \sim 2\pi \times 10$ MHz, the Doppler temperature $T_{\mathrm{D}} \sim 100$ μK. Further development of laser cooling led to achieving atomic temperatures below this limit by means of sub-Doppler, Raman, and velocity-selective cooling based on coherent population trapping (see review Ref. [12]). The usage of laser-cooled atomic ensembles in frequency standards and quantum information science are described in review Refs [13, 14].

To achieve ultra-low temperatures (nano- and femtokelvin), recourse is made to evaporative cooling of atoms in magnetic or optical traps [15, 16]. This technique is currently the standard way to obtain degenerate Bose and Fermi gases [17–19], which are widely used in various experiments, from the study of phase transition physics [20] to frequency standards [21] and gravimeters [22] operating on the principle of an atomic fountain.

Laser cooling has had a revolutionary impact on the field of frequency standards. Specifically, laser cooling of cesium atoms, whose transition is used to determine the second in the SI, led to the appearance of atomic fountains [23], which are an order of magnitude more accurate than the best beam systems [24]. No less an impact was exerted on optical standards: it became possible to replace atomic beams and gas cells with ultracold clouds. Low particle velocities in the cloud provide virtually unlimited interaction time with the ensemble and significantly reduce the contribution of the Doppler effect. Today, the requirements governing the instability of optical clocks are growing, which entails the development of new cooling methods to eliminate a number of small frequency shifts. In this paper, we describe some original aspects of laser cooling in optical clocks reliant on thulium atoms, whose development and implementation has been carried out at the Lebedev Physical Institute over the past decade.

It should be noted that progress in the development of optical clocks allows them to be used to solve a large number of fundamental and applied problems, and in some cases it is necessary to make compact and transportable devices. Neutral thulium atoms are a promising platform for such devices due to their low sensitivity to external conditions. A necessary step for constructing an optical clock based on neutral atoms is the characterization of frequency shifts caused by the radiation of the optical lattice. Since such frequency shifts depend on the motion of atoms in the optical lattice, i.e., on their temperature, their accurate measurement invites the preparation of atoms in the initial states of clock transitions at the lowest possible temperature.

2. Laser cooling in optical clocks

In modern optical clocks, laser cooling of atoms or ions is an integral part of the experiment. In the case of neutral-atom systems, the laser cooling and trapping of atoms in a magneto-optical trap (MOT) is the first step to ensure subsequent loading of atoms into an optical dipole trap at a magic wavelength [25]. When performing spectroscopy of an atomic transition in the Lamb–Dicke regime [26] and resolved sideband regime, the frequency shifts associated with linear Doppler effect and recoil effect are suppressed. However, deep laser cooling is still necessary to ensure control of the systematic frequency shift at a level of 10^{-18} rel. units. To eliminate the quadratic Doppler effect at this level, it is necessary to ensure that the velocity of atoms in the trap is less than 0.5 m s^{-1}, which for a Maxwellian distribution corresponds to a temperature of about 100 μK. It should be noted that, in ion optical clocks, a low temperature is also needed to reduce frequency shifts arising from micromotion in the radio frequency potential [27]. In turn, in optical clocks on neutral atoms, the need to operate at low temperatures stems from the sensitivity of the clock transition frequency to the vibrational quantum number along the axis of the optical lattice due to shifts arising from multipole polarizability and hyperpolarizability [28].

Since the distance between the vibrational levels of ions in radio frequency traps and atoms in optical lattices (along the lattice axis) is of the order of 100 kHz, the most commonly used method of laser cooling is the sideband-cooling technique [10, 29]. It is underlain by the excitation of an atomic transition with a decrease of vibrational quantum number (red sideband) and the subsequent return of the atom to the initial state through spontaneous decay without changing the vibrational number (due to operation in the Lamb–Dicke regime). Three cooling techniques at vibrational frequencies can be distinguished: (1) using a transition with a natural width of $\sim 1-10$ kHz, which provides a sufficiently fast spontaneous decay [28]; (2) a Raman transition using different levels of the hyperfine structure or magnetic sublevels of the same level [30, 31]; (3) excitation of a narrow clock transition on the red vibrational sideband with subsequent population transport [32]. In (2) and (3), the transporting radiation is used to return the atom to the initial state, which excites the atom to a short-lived level.

Cooling to the ground vibrational state is one of the stages of preparation of atoms in the best optical clocks which are under development in the world today. The inaccuracy of

such devices has reached the level of 10^{-18} rel. units [33, 34], while instability of 10^{-18} can be achieved in an averaging time of about one hour [35]. These characteristics are unattainable for the best microwave standards (atomic fountains), exceeding them by two orders of magnitude, which allows us to talk about redefining the second by 2030 [36]. These high characteristics allow us to use optical clocks in solving a wide range of problems, both fundamental and applied. Among the former, for example, are the search for violations of Lorentz invariance [37, 38], verification of the general relativity theory [39], and the search for dark matter [40, 41]. Among the applied tasks, mention can be made of the use of optical clocks in satellite navigation [42], relativistic geodesy [34, 43, 44], and synchronization of various processes [45].

Solving some tasks calls for the development of compact or transportable devices that can be used outside the laboratory. At present, such systems based on neutral atoms and ions are being developed worldwide [44, 46, 47]. The advantage of optical clocks based on neutral atoms is that a large number of particles (about 10^4) are simultaneously interrogated and statistical averaging occurs much faster than in the case of single ions. A significant disadvantage of such systems is the high sensitivity of neutral atoms to external disturbances, in particular, to thermal radiation in the environment. For example, the frequency shift of the clock transition in strontium atoms due to interaction with thermal radiation in the environment at room temperature ($T = 300$ K) is -2 Hz from the transition frequency, which corresponds to a shift in relative units of 5.5×10^{-15} [48]. While in the case of laboratory devices this problem can be solved by precise stabilization of the ambient temperature or by using cryogenic systems, in the case of transportable clocks it is difficult to use such methods. Therefore, at the moment, different atomic systems with a lower responsivity to the environment are being studied.

One such promising alternative is ensembles of neutral thulium atoms, which are being studied at the Lebedev Physical Institute [49, 50]. Interest in this system is due to the intrashell clock transition at a wavelength $\lambda = 1.14$ μm. As we showed in Ref. [51], the relative frequency shift of this transition due to thermal radiation of the environment is 2.3×10^{-18}, which corresponds to a transition frequency shift of less than 1 mHz. Interrogation of the clock transition between the central magnetic sublevels eliminates the frequency shift caused by the linear Zeeman effect, and the 'synthetic frequency' interrogation protocol allows us to suppress shifts related to the quadratic Zeeman effect [52]. Together, this has the effect that the total systematic frequency shift of thulium atoms is of the order of a mHz, which is a record low value for optical clocks on neutral atoms. The low value of the systematic shift allows achieving the required level of error without significantly complicating the design of the optical clock, which makes it compact and reliable.

One of the important steps in the development of optical clocks reliant on neutral atoms is the determination of frequency shifts caused by the radiation of the optical lattice. The frequency shift associated with the electric-dipole (E_1) polarizability can be eliminated by making an optical lattice at a 'magic' wavelength, when the dynamic polarizabilities of the upper and lower clock levels are equal [53]. However, when reaching an inaccuracy at the level of 10^{-17} rel. units, it becomes necessary to take into account the influence of high-order polarizabilities: electric-quadrupole (E_2) and magnetic-dipole (M_1) polarizabilities and hyperpolarizability [54, 55]. Using the concept of the so-called 'magic intensity' of the optical lattice allows one to choose the parameters (detuning from the magic wavelength and potential depth) of the optical lattice so that depth fluctuations introduce the smallest possible frequency uncertainty [28]. Successful implementation of this idea requires determination of the contributions of high-order polarizabilities with an accuracy that allows control of shifts at a level better than 10^{-17}. An additional complication is that, due to the difference in spatial dependences of the potentials responsible for the shifts associated with E_2/M_1 polarizabilities, the resulting frequency shift also depends on the motion of atoms in the optical lattice and, as a consequence, on their temperature. Therefore, for accurate characterization of such shifts, a high level of control over the motion of atoms is called for, i.e., their cooling to the ground vibrational state in the optical lattice.

Our previously implemented protocol for an thulium optical clocks in an optical lattice did not provide for cooling to the ground vibrational state. It included optical pumping of atoms to the central magnetic sublevel [56] and cooling of atoms by the sifting method due to a short-term decrease in the optical lattice depth [57]. This approach has several disadvantages. Atoms scatter photons in the course of optical pumping, resulting in their heating and loss from the lattice. Cooling by the sifting technique is based on the removal of hot atoms that are not retained in the optical lattice with a small potential depth, which also leads to losses. If we try to achieve lower temperatures in this way, the loss will increase. The lowest temperature we achieved by this method was $T \approx 3$ μK at a final lattice depth of 1000 E_{rec} and a minimum sifting depth of $\sim 80\, E_{\text{rec}}$. In this case, after the sifting procedure, fewer than 2% of the atoms trapped in the MOT would persist. In the case of a one-dimensional optical lattice, this temperature determines the Boltzmann distribution of atoms over the vibrational levels of the potential. To describe the population of the vibrational sublevel n_z along the z-axis of the optical lattice, in this paper we will use the notation $p_z(n_z)$. A more indicative parameter than the temperature in this case is the average vibrational number $n_z^{\text{avr}} = \sum_{n_z} n_z p_z(n_z)$. The temperature $T \approx 3$ μK for the Boltzmann distribution for the potential depths characteristic of our setup of $1000\, E_{\text{rec}}$ corresponds to the average vibrational number $n_z^{\text{avr}} \approx 0.5$. The relative frequency shift error associated with this cooling level can be estimated at 10^{-16}. To this end, we used typical values of high-order polarizabilities borrowed from work on strontium optical clocks [28]. Although in the case of thulium this estimate may be somewhat off, the value is almost an order of magnitude greater than the contribution of other systematic effects, so we need an improved atom preparation protocol that includes cooling to the vibrational ground state.

As shown in our earlier work [58], there is a cooling cyclic transition at a wavelength of 506.2 nm with a natural linewidth of 7.8 kHz in the thulium atom, which allows resolving sideband transition frequencies and using it for cooling (Fig. 1b). In this work, we describe an experimental study of the spectrum of this transition, the procedure of optical pumping, and subsequent cooling at sideband vibrational frequencies using it. Similar to previous studies on optical clocks with thulium atoms, after two stages of laser cooling in a magneto-optical trap, the atoms are recaptured

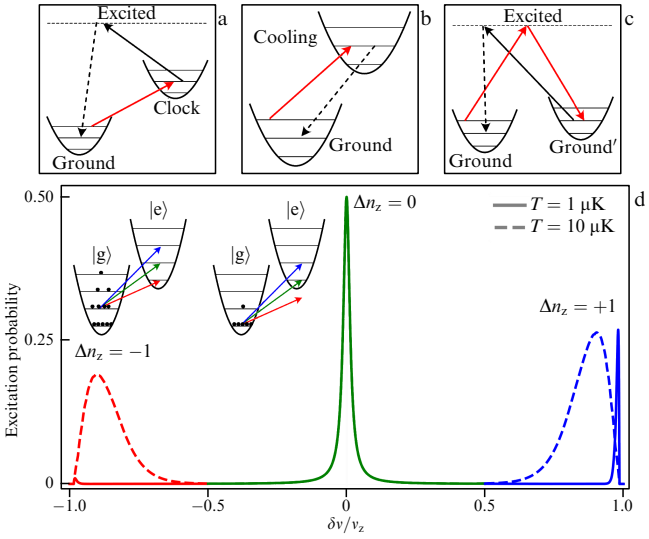

Figure 1. Different methods of laser cooling to vibrational ground state in an optical lattice. (a) Excitation of red vibrational sideband of clock transition with subsequent pumping of atoms to ground state via an intermediate short-lived level. Pumping is necessary because lifetime of excited state is too long for effective cooling. (b) Cooling using a spectrally narrow transition, whose spectral width, on the one hand, allows selective excitation of red vibrational sideband (red line) and, on the other hand, ensures fast spontaneous decay without changing the vibrational number (black line). (c) Raman transition between two (magnetic) sublevels of ground state with a decrease in the vibrational number by unity. (d) Characteristic transition spectrum in allowed sideband mode for two different temperatures of atomic ensemble. Dashed line shows spectrum for $T_z = T_r = 10$ μK — characteristic temperature of atomic ensemble after recapture of atoms from MOT into optical lattice. The number of atoms in ground vibrational state determines relative intensities of blue and red sidebands. Solid line corresponds to ensemble of atoms after-cooled further to $T_z = T_r = 1$ μK. Most atoms in this case are in ground vibrational state, which leads to almost complete disappearance of red sideband.

into an optical lattice at a wavelength of 1063.65 nm, which operates throughout the experiment. The following pulses of optical pumping and sideband cooling using the 506.2-nm transition are shown in Fig. 2 and will be described in this paper. Figure 2 also shows a diagram of the 506.2-nm laser beams used in this work. The 506.2-nm radiation was combined with the cooling radiation of the first and second stages of the MOT to the optical fiber that delivers the radiation to the system, so the beam configuration was equivalent to the classical six-beam configuration of the MOT. The beam radius was $w = 1$ cm at the intensity level of $1/e^2$. This configuration was used both to study the transition spectrum and to implement pumping and cooling. In this case, the beams traveling in the horizontal plane performed Doppler cooling in the radial direction of the optical lattice, and the beams traveling at an acute angle to the z-axis were used for cooling at side frequencies. The radiation at a wavelength of 1.14 μm was used to measure the sideband frequency spectrum of the clock transition to determine the atomic temperature.

3. Measurement of level polarizabilities for 506.2-nm transition

To implement laser cooling, it is necessary to ensure the spectral width of the laser emission line and its frequency stability at a level of less than 1/10 of the natural line width. For laser cooling of thulium atoms at the 506.2-nm transition with a natural line width of $\gamma = 7.8$ kHz, the laser frequency is stabilized by an ultrastable cavity [59], which made it possible to achieve an atomic temperature in the MOT below 1 μK [58].

For efficient cooling, it is important to use a cyclic transition, upon excitation of which the atom does not pass to other quantum states and does not escape from the cooling cycle. In the case of resolved Zeeman sublevels, such a role can be played by a transition between extreme magnetic sublevels (under the additional condition that there be no other probable decay channels). For the 506.2-nm transition in thulium, these conditions are satisfied by $|g, F = 4, m_F = -4\rangle \rightarrow |e, F = 5, m_F = -5\rangle$. To implement such a process, it is necessary to know the frequency of the required transition and make sure that no other transitions will be excited, which would disrupt the cyclicity of the cooling procedure. To construct a correct model describing the spectrum of the cooling transition for different experimental parameters, we experimentally studied the dependences of the Zeeman component frequencies on the value of the optical lattice potential.

To estimate the influence of the optical lattice, one can use an approximate model that describes the frequency shift of

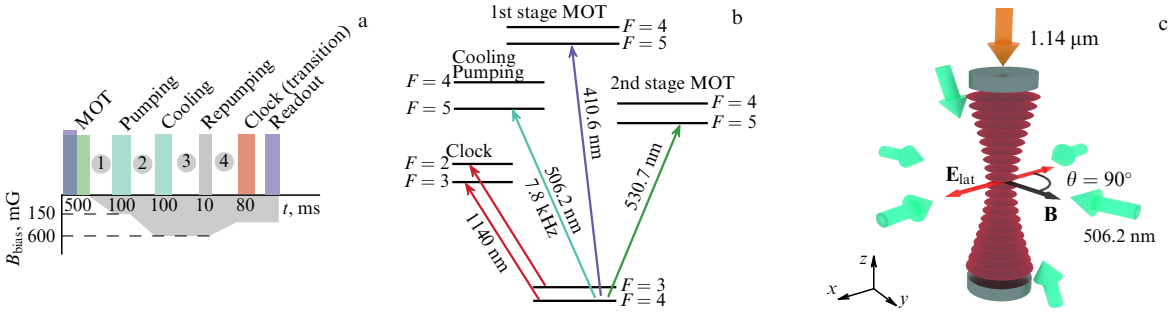

Figure 2. (a) Schematic diagram of pulses in the atom preparation protocol under development, (b) diagram of levels and optical transitions used, and (c) schematic diagram of laser beams in atom trapping region. MOT stage is implemented using 410.6-nm and 530.7-nm transitions, and pumping and cooling stage is implemented using 506.2-nm transition. Numbers 1–4 designate key time points in preparation and cooling cycles, which are discussed at length in the paper. Schematic diagram (c) shows polarization of optical lattice and driving magnetic field. Radiation at a wavelength of 1.14 μm is introduced along the optical lattice. Radiation at a wavelength of 506.2 nm is introduced with MOT beams in a classical six-beam configuration. Radial cooling is performed by beams lying in the horizontal plane, and a pair of beams directed at an acute angle to the z-axis is used for cooling at side frequencies.

each of the Zeeman sublevels $|i, F, m_F\rangle$ of a certain level $|i, F\rangle$ in relation to the intensity I of the external linearly polarized radiation of the optical lattice. For practical use in all formulas where the intensity of the optical lattice is present, we will rewrite it in terms of the lattice depth U for the central magnetic sublevel of the ground state $|g, F = 4, m_F = 0\rangle$ expressed in units of recoil energy $E_{rec} = h^2/2m\lambda^2 = h\nu_{rec} = h \times 1.043$ kHz. The advantage of using the lattice depth is that it can be determined experimentally from the spectrum of the clock transition, while the radiation intensity and polarizability in atomic units are related to each other, and their errors are usually determined from direct intensity measurements by methods unrelated to spectroscopy. Instead of polarizability in atomic units α, in this case, a transition occurs to polarizability $\bar{\alpha} = \alpha/\alpha_0$ in units of polarizability of the ground state of the clock transition $|g, F=4, m_F=0\rangle$: $\alpha_0 = \alpha_g^s + 5/14\alpha_g^t$. The dependence of the energy of the state $|i, F, m_F\rangle$ of an atom in a constant external magnetic field and in the potential of the optical lattice is of the form

$$E_{i,F,m_F} = E_{i,F} + m_F g_F^i \mu_B B - \left(\bar{\alpha}_{i,F}^s + \frac{3\cos^2\theta - 1}{2} \frac{3m_F^2 - F(F+1)}{F(2F-1)} \bar{\alpha}_{i,F}^t\right) U. \quad (1)$$

Here, B is the magnetic induction, μ_B is the Bohr magneton, θ is the angle between the magnetic field direction and the polarization of the optical lattice, which is equal to 90° throughout the paper, $|i\rangle$ denotes the level under study, which can be either the ground $|g\rangle$ or the upper $|e\rangle$ level of the 506.2-nm cooling transition. $E_{i,F}$ is the unshifted energy of the $|i, F\rangle$ level, g_F^i is its Lande factor.

The dynamic scalar and tensor polarizabilities of the ground state of thulium atoms at a wavelength of $\lambda = 1064$ nm were measured earlier [60] and are $\alpha_g^s = 167(25)$ a.u. and $\alpha_g^t = -4(1)$ a.u., respectively (in units of the ground state polarizability, they are $\bar{\alpha}_g^s = = 1.009(2)$ and $\bar{\alpha}_g^t = -0.024(6)$, respectively). The Lande factors for both levels are also known [61–63] and are $g_J^g = 1.141189(3)$ and $g_J^e = 1.29(1)$, which corresponds to $g_F^g = 0.998540(3)$ and $g_F^e = 1.16(1)$ for the hyperfine components $|g, F = 4\rangle$ and $|e, F = 5\rangle$, respectively. To construct the model, it only remains to measure the dependences of the energies of the upper level of the cooling transition on the depth of the optical lattice.

In our experiments, we have the capability to prepare atoms on the extreme and central magnetic sublevels of the ground state. This procedure was described at length in Refs [56, 64]; another new method will be described in this paper. The number of atoms on each of these sublevels was measured in the Stern–Gerlach experiment [65]: current was applied to the coils in the anti-Helmholtz configuration, and, after 20 ms (the characteristic time of magnetic field settling), the radiation producing the optical lattice was switched off. After an expansion time $\tau = 15$ ms, a picture of the cloud was taken, and the resulting image was approximated by the sum of several Gaussians. The relative amplitude of each Gaussian is related to the number of atoms on a specific magnetic sublevel; therefore, the ratio of the 'amplitude' of the sublevel under study to the sum of the 'amplitudes' is taken as the degree of depolarization. Figure 3a shows a typical image obtained as a result of such an experiment.

By scanning the frequency of laser radiation at a wavelength of 506.2 nm, we obtain the excitation spectrum of the transitions under study proceeding from measurements

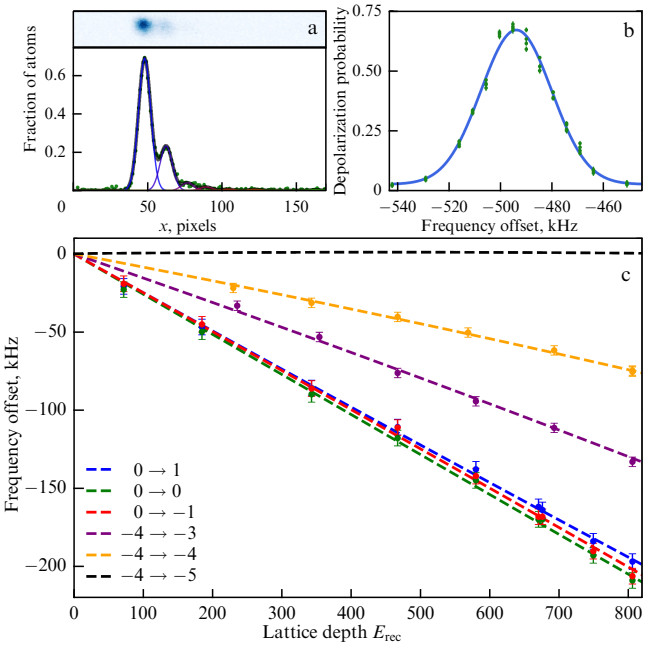

Figure 3. (a) Picture of the cloud obtained in Stern–Gerlach experiment after depolarization of atoms from sublevel $m_F = -4$ and approximation of resultant image by the sum of Gaussians corresponding to all sublevels of ground state. (b) Example of a spectral line obtained in the experiment. Frequency offset is measured from position of transition unperturbed by the magnetic field and field of the optical lattice. (c) Difference in frequencies of transitions between different magnetic sublevels of upper and lower states (magnetic numbers are given in inset) as functions of depth of optical lattice potential in units of recoil energy E_{rec}. Frequency offsets are measured from frequency of transition between corresponding magnetic sublevels unperturbed by the optical lattice. Zeeman frequency shift is subtracted. Dotted curves correspond to approximation of these frequencies using model described in the text. Only the model is presented for transition between extreme magnetic sublevels $-4 \to -5$.

of the fraction of depolarized atoms. Figure 3c shows the data obtained for transitions $\sigma^{\pm}, \pi$ from the level $|g, F = 4, m_F = 0\rangle$ and for transitions σ^+, π from the level $|g, F = 4, m_F = -4\rangle$. The transition σ^- from the extreme level corresponding to $|g, F = 4, m_F = -4\rangle \to |e, F = 5, m_F = -5\rangle$ is cyclic and does not depolarize atoms. The effect of excitation of this transition can be detected only by the heating and loss of atoms, but this leads to an asymmetric shape of the excitation spectrum line and complicates determining the line center.

The total power of the radiation introduced into the system was $P \approx 250$ μW, which corresponds to the saturation parameter $s = 30$. The atoms–radiation interaction time was $\tau = 5$ ms, which is far longer than the typical time an atom takes to scatter a photon on this transition.

We measured the dependence of the frequency of each of the accessible transitions on the optical lattice depth for a magnetic field of 340 mG. The experimental results showed a difference between the model defined by formula (1) and the experimental points. According to the model, the frequencies of $\sigma^{\pm}$ transitions from the central magnetic sublevel $|g, m_F = 0\rangle \to |e, m_F = \pm 1\rangle$ should shift equally with a change in the optical lattice depth. However, an appreciable difference is observed in the experiment (blue and red curves in Fig. 3c).

We attribute this difference to the fact that, under our experimental conditions, when the angle between the magnetic field and the lattice polarization is $\theta = 90°$, mixing of the upper-level states occurs. The construction of a more complex

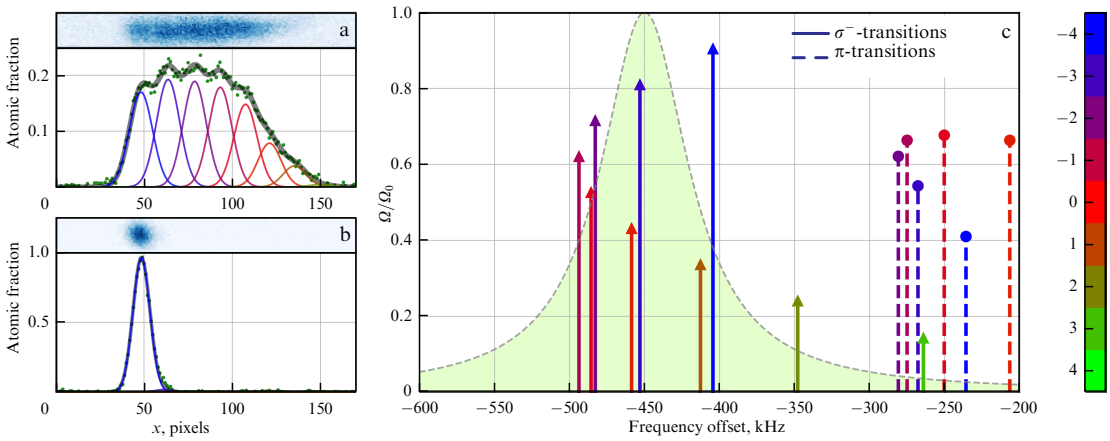

Figure 4. (a) Picture of the cloud obtained in Stern–Gerlach experiment after recapture of atoms from MOT into the optical lattice. Image is approximated by sum of Gaussians corresponding to atoms in all sublevels of ground state. Atoms are distributed almost uniformly over sublevels $m_F = -4, \ldots, 0$, while there are practically no atoms in sublevels $m_F = +3, +4$. (b) Photograph of cloud obtained in Stern–Gerlach experiment after optical pumping. 98% of atoms are concentrated in extreme magnetic sublevel. (c) Transition frequencies in the mode of a weak magnetic field (150 mG was chosen to implement optical pumping). Solid lines denote frequencies of σ^- transitions, and dotted lines denote frequencies of π transitions. Magnetic sublevels of ground state from which the transition occurs are shown in color. In this mode, most σ^- transitions can be excited by a single high-power pulse. For example, background line profile corresponds to power-broadened laser radiation with saturation parameter $s = 20$.

model based on diagonalization of the Hamiltonian, finding its eigenvectors, and expanding them into states of the 'ordinary' magnetic sublevels $|F, m_F\rangle$, according to Ref. [66], explained the observed difference in slopes, but led only to minor corrections to the polarizabilities.

Results of experimental data approximations using formula (1) with the inclusion of the effect of state mixing are shown by dashed lines in Fig. 3. The resultant values of the reduced polarizabilities were $\bar{\alpha}_e^s = 1.146(4)$ and $\bar{\alpha}_e^t = 0.283(15)$, which corresponds to $a_e^s = 190(30)$ at. units and $\alpha_e^t = 47(7)$ at. units. The errors in the polarizabilities in relative units were obtained by approximating the experimental data presented in Fig. 3 and are determined mainly by the statistical scatter of the points. The errors in the absolute values are associated with the uncertainty of the polarizability of the ground state, whose determination calls for accurate measurements of the intensity of the radiation producing the optical lattice. To investigate the spectrum of magnetic sublevels of the 506.2-nm transition in this work, we are concerned only with the relative $\bar{\alpha}$ values.

The measured polarizability values allow us to distinguish two different operating modes involving the 506.2-nm transition. In a strong magnetic field ($B > 500$ mG), the transition frequencies are determined mainly by the Zeeman effect, and the shift due to the Stark effect is only a small correction, so, by and large, the picture does not change. When using weaker magnetic fields ($B < 200$ mG), the contribution of the Stark effect to the transition frequency shifts becomes comparable to the contribution of the Zeeman effect. The frequencies of some transitions in this operating mode are depicted in Fig. 4. Intermediate values of the magnetic field were not used in the experiment due to the presence of Feshbach resonance for the state $|g, F{=}4, m_F{=}-4\rangle$ in a magnetic field $B \approx 430$ mG [67], approaching which causes a significant loss of atoms in the course of cooling.

4. Optical pumping

Implementing laser cooling calls for concentrating the atoms in one of the extreme magnetic sublevels from which the cyclic cooling transition can be excited. This can be achieved by working with a MOT with a large detuning of the cooling radiation from the resonance [64], but this leads to a bowl-shape MOT, entailing a sharp reduction of the overlap region with the optical lattice and the consequential large loss of atoms during recapture. After recapture from a compact MOT, the atomic cloud is not polarized (Fig. 4a), which generates a need to pump the atoms to the extreme magnetic sublevel. As already noted, this can be achieved by the optical pumping method at the 418-nm transition [56] using σ^- polarized radiation. The advantages and disadvantages of this method are related to the natural linewidth of this transition, which is 10 MHz. On the one hand, this allows us to simultaneously address all magnetic sublevels of the ground state in the excitation of the σ^- transition, since the separation due to the Zeeman effect usually amounts to hundreds of kHz. On the other hand, this entails heating of the atoms due to multiple spontaneous decay events in the course of optical pumping. An additional disadvantage of this method is the need for an additional laser system.

In this paper, we propose that the 506.2-nm transition under study be employed both for optical pumping and for cooling. For optical pumping, the same beam configuration was used as for polarizability studies: 506.2-nm radiation was combined with MOT beams in a classical six-beam configuration. The natural spectral width of the transition is 7.8 kHz, which is smaller than the characteristic Zeeman splitting of levels. Consequently, simultaneous excitation of transitions from all magnetic sublevels may not occur.

The relatively high value of the tensor polarizability of the upper level $|e\rangle$ of the 506.2-nm transition allows us to select the experimental parameters so that the frequencies of the σ^- transitions from different magnetic sublevels of the ground state are close. This significantly simplifies the procedure of optical pumping and selection of the optimal parameters. To this end, the depth of the optical lattice potential $U = 1000\, E_{rec}$ and the magnetic field induction $B = 150$ mG were chosen. The frequencies of the σ^- and π transitions from all sublevels of the ground state in this configuration, as well as the offset from the resonance of the pump radiation frequency, are shown in Fig. 4c. The atoms, initially located

in the sublevels $m_F = -3, \ldots, +2$, are pumped to the target extreme sublevel $m_F = -4$ by one powerful pulse. Note that the atoms from the sublevels $m_F = +4, +3$ can be pre-pumped using individual pulses. However, since initially there are hardly any atoms in these magnetic sublevels (Fig. 4a), this is not necessary.

The parameters of the cooling beams are similar to those used for the polarizability study: $P \approx 250$ μW ($s = 30$). The pulse duration was $\tau = 50$ ms. The resultant polarization purity is $\eta \approx 98(2)\%$ (Fig. 4b) without detectable loss of atoms from the optical lattice. The remaining 2% of unpumped atoms are concentrated mainly in the magnetic sublevel $|g, F = 4,\ m_F = -3\rangle$, which can be attributed to depolarization during switching on the magnetic field for the Stern–Gerlach experiment, nonresonant excitation of the π transition from the magnetic sublevel $|g, F = 4, m_F = -4\rangle$, or the previously mentioned effect of state mixing [66].

5. Cooling

The laser cooling procedure in an optical lattice differs from that in a MOT. The main difference is the quantization of the atomic motion along one of the directions (or several in the case of multidimensional lattices), which has the effect of splitting the spectral lines into a large number of components associated with transitions between different vibrational sublevels. Laser cooling in this case consists in the excitation of transitions with a decrease in the number of the vibrational sublevel (Fig. 5b). Along the axes, the motion along which is not quantized or this quantization is not so pronounced, conventional Doppler cooling can be implemented with a correction for the influence of the Stark effect.

The type of spectrum of the transition under study with the separation of vibrational sublevels is determined by the influence of the radiation of the optical lattice on the energies of the levels, i.e., their polarizabilities. The energy of an atom in a certain state i on the vibrational sublevel n_z of the optical lattice is defined by the formula [57]

$$E^i_{n_z} = E^i + h\nu^i_z\left(n_z + \frac{1}{2}\right) - h\nu_{\text{rec}}\left(n_z^2 + n_z + \frac{1}{2}\right), \qquad (2)$$

where E^i is the energy level according to formula (1), $h\nu^i_z = 2(U^i_0 E_{\text{rec}})^{1/2}$, and U^i_0 is the potential depth for an atom in state i, which is determined by the term proportional to the potential depth for the ground state U (the third term in expression (1)). For close values of polarizability of two levels, the potential depths will be similar and the spectrum will assume a characteristic form with the carrier and side frequencies (Fig. 5a). In this case, for levels with different polarizabilities, the second term $h\nu^i_z$ will be different and the side frequency spectrum may differ greatly from the classical one; accordingly, transitions with different values of Δn_z will be mixed (Fig. 5b).

The difference in the polarizabilities of the levels for the cooling transition is close to zero, which has a positive effect on the cooling procedure for two reasons. First, since the cooling transition frequency is hardly dependent on the lattice depth (the transition frequency shift at a lattice depth of $U = 1000E_{\text{rec}}$ is 1.5 kHz, which is less than the natural line width), effective Doppler cooling of atoms is possible, similar to Doppler cooling in free space. Second, the experimental conditions allow effective cooling of atoms along the direction of propagation of the optical lattice (hereinafter referred to as the axial direction, the Oz axis) with one high-power pulse. Such a pulse (Fig. 5a) will excite transitions with a decrease in the vibrational number from all sublevels without affecting other transitions.

In our laboratory, there are two experimental setups of thulium optical clocks. The laser beam geometries in them are different. In the first setup, one of the MOT beams is directed at a small angle to the z-axis, along which the optical lattice is formed, while the other two propagate in the horizontal xy plane. This configuration allows efficient cooling of atoms in

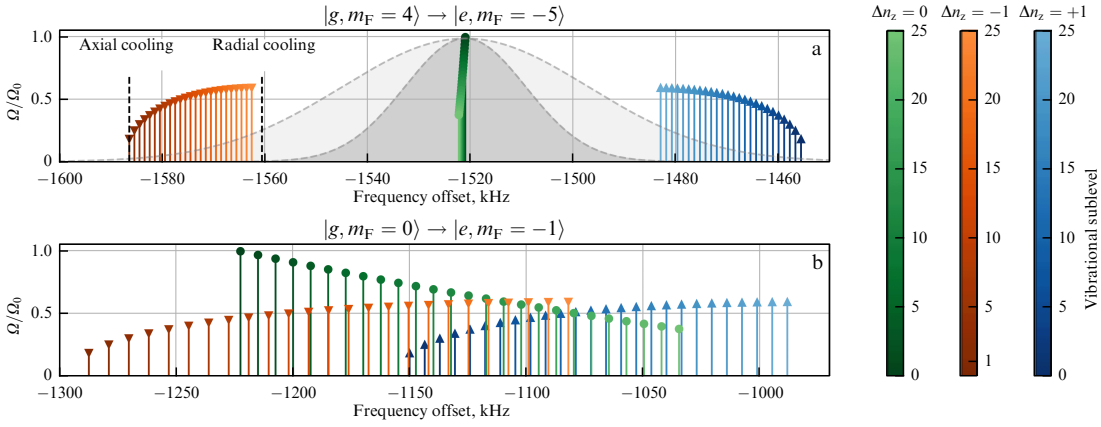

Figure 5. Frequencies of transition between different vibrational sublevels for two different components of the transition (cooling $|g, m_F = -4\rangle \rightarrow |e, m_F = -5\rangle$, and transition that could be used to blow away hot atoms from $m_F = 0$: $|g, m_F = 0\rangle \rightarrow |e, m_F = -1\rangle$). Frequencies are given for experimental conditions: lattice depth $U = 1000E_{\text{rec}}$, magnetic field $B = 600$ mG. Frequencies in graphs are measured from frequency of unperturbed transition. Frequencies of transitions with a decrease in the vibrational number by one are shown in red, those without a change in the vibrational number, in green, and those with an increase by one, in blue. Shade of color indicates vibrational sublevel from which the transition is excited. (a) For a cooling transition, Doppler broadening is shown before cooling (light gray profile) and after cooling (dark gray profile), corresponding to temperatures $T_r = 13$ μK and $T_r = 3$ μK, respectively. Black dotted line shows frequencies of cooling radiation pulses. (b) Frequencies of transitions between different vibrational sublevels of the optical lattice for transition from central magnetic sublevel. Efficient cooling similar to (a) would be impossible here. Possible, however, is the final removal of atoms that are not in the zero vibrational sublevel: by exciting transitions with a decrease in the vibrational number, we will reach a state where all atoms which are not in zero vibrational sublevel in optical lattice potential will either fall into ground vibrational state or leave central magnetic sublevel and will be removed from lattice in the process of purification of atomic polarization.

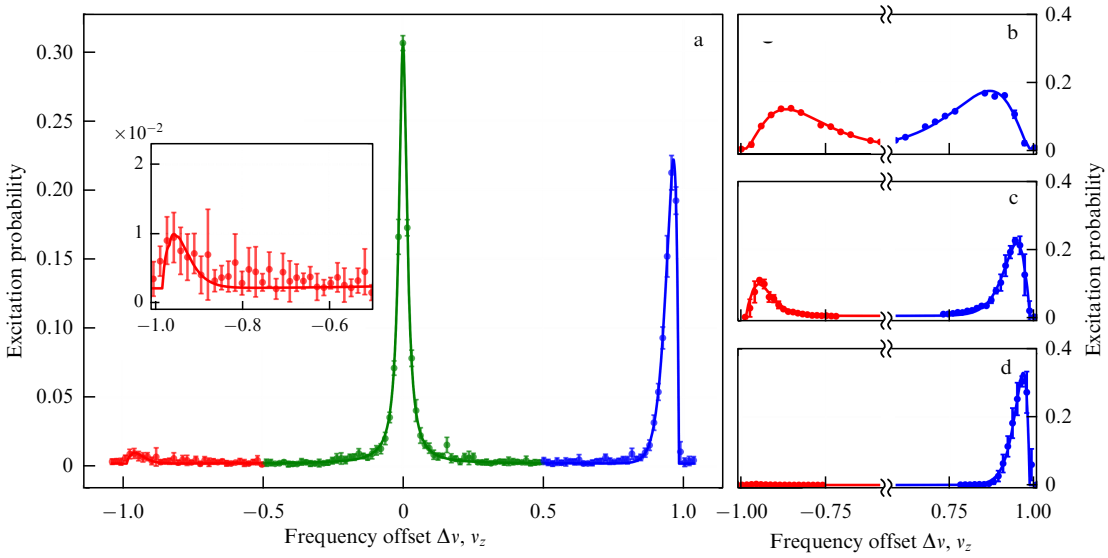

Figure 6. Spectroscopy of sideband vibrational frequencies of 1.14 μm-clock transition in different cooling modes: (a) after repumping to central magnetic sublevel. In plots, $\nu_z \approx 70$ kHz, $\nu_{\text{rec}} \approx 73$ kHz; (b) without cooling; (c) only with radial cooling; (d) with total cooling.

both directions (axial and radial) without additional changes. In the second setup, one beam is directed along the x-axis, while the other two propagate in the yz plane at an angle of 45° to the z-axis. In such a configuration, during cooling along the z-axis, upon absorption of a photon, a change in the momentum in the radial direction occurs, and a competition of cooling effects in the radial and axial directions is possible. For this reason, in the second experimental setup, there is an additional beam of cooling radiation directed along the z-axis.

The following parameters were chosen to implement cooling: lattice depth $U = 1000\,E_{\text{rec}}$, $B = 600$ mG. The chosen lattice depth is characteristic of our experiment and can be lowered if necessary for subsequent interrogation of the clock transition. The choice of magnetic field is related to the presence of Feshbach resonances for the extreme magnetic sublevel at points of 430 and 800 mG [67]. The region $B < 300$ mG corresponds to a smaller separation of the transition components with σ^+, π-polarizations, i.e., a higher probability of nonresonant excitation of unwanted transitions.

Cooling is effected by two pulses of duration $\tau = 50$ ms for cooling in the radial and axial directions, respectively. The characteristic frequency offsets from the unperturbed resonance for each of the pulses are depicted in Fig. 5 and are ≈ -1560 kHz for cooling in the radial direction and ≈ -1590 kHz for cooling in the axial direction, which corresponds to offsets ≈ -40 kHz and ≈ -70 kHz from the carrier frequency. The characteristic powers for these pulses are about 200 μW, which corresponds to the saturation parameter $s \approx 25$.

The optical lattice is formed at the magic wavelength, so realized for the central magnetic sublevel is the case of close polarizabilities, and the transition spectrum consists of a pronounced carrier and two side bands. The tensor polarizability of the clock transition is fairly low, so a similar situation is realized for a clock transition from the extreme magnetic sublevel. To measure both the axial and radial temperatures of the atoms, we performed a spectroscopy of the vibrational sidebands of the clock transition [57]. The resultant spectrum was approximated by a model

Table. Atomic temperatures (T_z, T_r) and average vibrational numbers n_z^{avr} at different stages of experiment.

Spectrum	T_z, μK	T_r, μK	n_z^{avr}	p_z^0
Without cooling (b)	7.8(3)	19.0(3)	1.94(8)	0.34(1)
Radial cooling (c)	4.6(3)	6.4(2)	0.76(6)	0.57(2)
Total cooling (d)	0.76(2)	4.21(10)	0.0097(15)	0.9904(15)
After transfer (a)	3(2)*	3.48(10)	0.07(5)	0.96^{+3}_{-6}

Last column gives probability of detecting an atom in zero vibrational sublevel p_z^0.
First column in parentheses contains links to corresponding spectra in Fig. 6. Given in parentheses for each of the values is confidence interval 1σ obtained from approximation.
* In after-transfer case (a), temperature of residual, uncooled ensemble of atoms in two-temperature distribution is indicated (see text). Probability p_z^0 and average vibrational number n_z^{avr} describe entire distribution.

describing the probability of excitation of transitions at vibrational sidebands spectra, taking into account the distribution of atoms over the vibrational sublevels of the optical lattice and the radial temperature of the atoms. This method is described at length in Refs [57, 68]. Therefore, the method of measuring the temperature by side vibrational frequencies was also used to optimize cooling in the extreme sublevel.

The cooling results in the form of sideband spectra are shown in Fig. 6 and in the Table. Each experimental point on the plot is indicated with an error associated with the fluctuation of the number of atoms at constant experimental parameters, and the errors presented in the Table correspond to the confidence 1σ interval of the result of the approximation of the vibrational sidebands by the theoretical model. Among the results, the spectrum measured before cooling in the optical lattice is presented for comparison, which corresponds to point in time (1) or (2) in Fig. 2. To illustrate the cooling operation, also depicted is the spectrum measured after Doppler cooling in the radial directions, which corresponds to the point in time 'cooling' in Fig. 2. In this case, a decrease in both (axial and radial) temperatures occurs, but

the average vibrational number still remains rather large. Finally, full sideband cooling effectively cools the atoms in the axial direction, only slightly lowering the radial temperature.

The axial temperature of the atoms attained at this stage (point in time (3) in Fig. 2) was 0.8 μK, which corresponds to an average vibrational number $n_z \approx 0.01$. On the graph, this manifests itself in the almost complete disappearance of the red vibrational sideband (red points in Fig. 6c). The decrease in temperature in the radial direction is less pronounced. It is noteworthy that, for measuring polarizabilities and operating optical clocks, the radial temperature is not as critical a parameter as the temperature along the axial direction. Following the formulas in Ref. [28], one can see that the radial temperature only changes the scale of the depth of the optical lattice potential by a few percent without noticeable changes in the frequency shift.

6. Repumping to central magnetic sublevel

The result of cooling the atoms to the average vibrational number $n_z^{\text{avr}} = 0.01$ corresponds to the level of operation of optical clocks in laboratories, where relative frequency errors at the level of 10^{-18} have been achieved. In our case, we approached $n_z^{\text{avr}} = 0.01$ at the extreme magnetic sublevel, but, for the operation of an optical clock on thulium atoms, the population must be transferred to the central magnetic sublevel $m_{\text{F}} = 0$.

In the case of optical clocks on other atoms, the task of transferring atoms to the central magnetic sublevel is infrequently encountered. Usually, either the two extreme sublevels are used (as with ^{87}Sr, for instance), or the central magnetic sublevel is the only one, which is true for atoms with $F = 0$ in the ground state. In our work, this problem does arise, and the method of preparing states using radiation at a wavelength of 418 nm [56] used in previous studies entails heating the atoms, making the preceding laser cooling to the ground vibrational level meaningless.

To pump atoms from $m_{\text{F}} = -4$ to $m_{\text{F}} = 0$, two methods were used. In one setup, the pumping was accomplished by exciting radio-frequency transitions between the Zeeman sublevels of the ground state. The characteristic frequencies of such transitions under our experimental conditions ($U = 1000E_{\text{rec}}$, $B = 600$ mG) were $\nu \approx 800$ kHz and differed from each other by about $\delta\nu \approx 30$ kHz due to the tensor polarizability of the $|g, F = 4\rangle$ level. To excite these transitions, a signal up to 0.5 W in power was fed to a homemade antenna. Even small fluctuations in the magnetic field in the setup lead to significant difficulties in exciting coherent π-pulses between the Zeeman sublevels, so instead we used a high-power 10-ms-long pulse, whose frequency was scanned in the range of 13 kHz, which covers all the required transitions between magnetic sublevels. As a result, approximately $\eta = 30\%$ of the initial number of atoms found themselves in the required sublevel $m_{\text{F}} = 0$.

The design of the second experimental setup did not allow the use of this technique: the characteristic distance from the antenna to the region of atom capture in this system turned out to be significantly greater than in the first one, which significantly reduced the efficiency of transition excitation. To implement the pumping of atoms in this setup, we used the previously mentioned phenomenon of state mixing, which leads to the possibility of exciting the transition $|g, m_{\text{F}} = -4\rangle \rightarrow |e, m_{\text{F}} = -1\rangle$, after which some of the atoms decay into $|g, m_{\text{F}} = 0\rangle$. To excite this pulse, use was made of an additional beam of σ^+ polarized radiation directed along the x-axis of the setup with a radius of $w = 1$ mm. The characteristic power in the beam was $P = 100$ μW, which corresponds to the saturation parameter $s \approx 800$. Such an intensity is necessary, because, in the operating mode ($B = 600$ mG), the effect of state mixing is suppressed, with the result that the transition $|g, m_{\text{F}} = -4\rangle \rightarrow |e, m_{\text{F}} = -1\rangle$ turns out to be much weaker than conventional transitions. The excitation duration was $\tau = 10$ ms, and the radiation frequency was tuned to the red side of the resonance to reduce the heating of the atoms. As a result, approximately $\eta = 20\%$ of the initial number of atoms ended up in the required sublevel $m_{\text{F}} = 0$.

In both cases, the final temperature of the atoms was somewhat higher than that in the initial extreme magnetic sublevel (see Fig. 6). The main reason for this is the nonpumped atoms, which did not participate in the cooling cycle. Figure 6 shows the characteristic spectrum obtained after pumping to $m_{\text{F}} = 0$, which is nicely approximated by a two-temperature distribution: the majority ($> 95\%$) of the atoms are at $n_z = 0$, and a small fraction is distributed over vibrational sublevels with a Boltzmann distribution with a temperature of 3 μK. In the case of the second setup, pumping can also lead to some heating due to the scattering of one photon, but the characteristic temperatures in it are at approximately the same level as in the first one.

In the future, we plan to remove atoms from a nonzero vibrational sublevel using a short laser pulse tuned in frequency to the red vibrational band of the transition with $\sigma^{\pm}$ polarization. Atoms in the ground vibrational state will hardly scatter any photons, while the rest will either lose one vibrational quantum as a result of photon scattering or leave the central magnetic sublevel and will be removed from the optical lattice in the course of subsequent purification of the polarization of the atomic cloud. The frequencies of the transition components $|g, F = 4, m_{\text{F}} = 0\rangle \rightarrow |e, F = 5, m_{\text{F}} = -1\rangle$ between different vibrational sublevels of the optical lattice are depicted in Fig. 5b.

It can be seen that the removal of atoms by this technique is possible only from low-lying vibrational sublevels: beginning with a certain vibrational sublevel, in the excitation of transitions with a change in the vibrational number by −1, transitions without a change in the vibrational number will also be excited, which will lead to heating of the atoms and depolarization, including in the ground vibrational state. On the other hand, at characteristic temperatures of the residual ensemble of atoms $T \approx 3$ μK, most of them are concentrated on the first few vibrational sublevels, which makes the implementation of this method possible.

7. Conclusions

In a study dedicated to the 55th anniversary of the foundation of the leading scientific institute in the field of laser spectroscopy and atomic and molecular optics — ISAN — we outlined some original approaches to deep cooling of thulium atoms to the ground vibrational state in an optical lattice. Despite the fact that similar experiments were performed by other world leaders developing precise optical frequency standards on strontium and ytterbium atoms, the specificity of the levels and transitions in the thulium atom required special methods and algorithms. As a result, we experimentally implemented laser cooling on the spectrally narrow 506.2-nm transition up to the value of the radial vibrational

quantum number of 0.01 in the extreme magnetic sublevel, which corresponds to sub-μK temperatures. After transfer to the central magnetic sublevel, the temperature increases slightly: prepared in the initial states of the clock transition are $N \approx 2 \times 10^4$ thulium atoms with an average vibrational number $n_z^{\text{avr}} < 0.1$. The studies performed are an important step towards overcoming the barrier of relative instability of 10^{-17}, which is our immediate goal [69].

It should be noted that work on developing compact clocks is also being carried out at ISAN: colleagues are successfully developing a technology for trapping atoms on a chip [70]. A combination of various technologies, such as atomic chips [70], integrated photonics [71, 72], compact laser systems [73, 74], and chip combs [75], opens up completely new prospects in the field of making transportable systems, allowing us to talk about a total system volume of about 1 liter. On the one hand, the small size of the system leads to a decrease in sensitivity to vibrations and facilitates temperature stabilization. However, as noted in the text, additional disturbances arise, including due to the approach of atoms to the surface of the chip or chamber. It is necessary to search for those atomic systems that are the least sensitive to the combination of these disturbances, which is partly the concern of our study. Perhaps the combination of the ISAN chip trap and the methods developed at LPI will make it possible to make compact and accurate next-generation optical clocks in the near future.

The study was supported by the Russian Science Foundation (RSF) under grant no. 21-72-10108.

References

1. Basov N G, Prokhorov A M *Usp. Fiz. Nauk* **57** 485 (1955)
2. Basov N G, Letokhov V S *Sov. Phys. Usp.* **11** 855 (1969); *Usp. Fiz. Nauk* **96** 585 (1968)
3. Letokhov V S, Chebotaev V P *Printsipy Nelineinoi Lazernoi Spektroskopii* (Principles of Nonlinear Lazer Spectroscopy) (Moscow: Nauka, 1975)
4. Lebedew P *Astrophys. J.* **31** 385 (1910) https://doi.org/10.1086/141769
5. Lukishova S, Masalov A, Zadkov V *Europhys. News* **50** (4) 15 (2019)
6. Frisch R *Z. Phys.* **86** 42 (1933) https://doi.org/10.1007/BF01340182
7. Hänsch T W, Schawlow A L *Opt. Commun.* **13** 68 (1975)
8. Dehmelt H G *Bull. Am. Phys. Soc.* **20** 60 (1975)
9. Andreev S V et al. *JETP Lett.* **34** 442 (1981); *Pis'ma Zh. Eksp. Teor. Fiz.* **34** 463 (1981)
10. Neuhauser W et al. *Phys. Rev. Lett.* **41** 233 (1978)
11. Letokhov V S, Minogin V G *Phys. Rep.* **73** 1 (1981)
12. Balykin V I *Phys. Usp.* **52** 275 (2009); *Usp. Fiz. Nauk* **179** 297 (2009)
13. Ryabtsev I I et al. *Phys. Usp.* **59** 196 (2016); *Usp. Fiz. Nauk* **186** 206 (2016)
14. Taichenachev A V, Yudin V I, Bagayev S N *Phys. Usp.* **59** 184 (2016); *Usp. Fiz. Nauk* **186** 193 (2016)
15. Adams C S et al. *Phys. Rev. Lett.* **74** 3577 (1995)
16. Ketterle W, Van Druten N J *Adv. Atom. Mol. Opt. Phys.* **37** 181 (1996) https://doi.org/10.1016/S1049-250X(08)60101-9
17. Turlapov A V *JETP Lett.* **95** 96 (2012); *Pis'ma Zh. Eksp. Teor. Fiz.* **95** 104 (2012)
18. Chapovsky P L *JETP Lett.* **95** 132 (2012); *Pis'ma Zh. Eksp. Teor. Fiz.* **95** 148 (2012)
19. Onofrio R *Phys. Usp.* **59** 1129 (2016); *Usp. Fiz. Nauk* **186** 1229 (2016)
20. Diehl S et al. *Nature Phys.* **4** 878 (2008)
21. Wynands R, Weyers S *Metrologia* **42** S64 (2005)
22. Peters A, Chung K Y, Chu S *Metrologia* **38** 25 (2001)
23. Weyers S et al. *Metrologia* **38** 343 (2001)
24. Bauch A et al. *IEEE Trans. Instrum. Meas.* **36** 613 (1987)
25. Katori H, Ido T, Kuwata-Gonokami M *J. Phys. Soc. Jpn.* **68** 2479 (1999)
26. Dicke R H *Phys. Rev.* **89** 472 (1953)
27. Keller J et al. *J. Phys. Conf. Ser.* **723** 012027 (2016)
28. Ushijima I, Takamoto M, Katori H *Phys. Rev. Lett.* **121** 263202 (2018)
29. Perrin H et al. *Europhys. Lett.* **42** 395 (1998)
30. Chen J-S et al. *Phys. Rev. Lett.* **118** 053002 (2017)
31. Seck C M et al. *Phys. Rev. A* **93** 053415 (2016)
32. Zhang X et al. *Phys. Rev. Lett.* **129** 113202 (2022)
33. Bothwell T et al. *Metrologia* **56** 065004 (2019)
34. McGrew W F et al. *Nature* **564** 87 (2018)
35. Nicholson T L et al. *Phys. Rev. Lett.* **109** 230801 (2012)
36. Dimarcq N et al. *Metrologia* **61** 012001 (2024)
37. Sanner C et al. *Nature* **567** 204 (2019)
38. Kostelecký V A, Vargas A J *Phys. Rev. D* **98** 036003 (2018)
39. Takamoto M et al. *Nat. Photon.* **14** 411 (2020)
40. Savalle E et al. *Phys. Rev. Lett.* **126** 051301 (2021)
41. Wcisło P et al. *Nat. Astron.* **1** 0009 (2017)
42. Giorgi G et al. *Adv. Space Res.* **64** 1256 (2019)
43. Lisdat C et al. *Nat. Commun.* **7** 12443 (2016)
44. Grotti J e al. *Nature Phys.* **14** 437 (2018)
45. Clivati C et al. *Sci. Rep.* **7** 40992 (2017)
46. Cao J et al. *Appl. Phys. B* **123** 1 (2017)
47. Semerikov I A et al. *Bull. Lebedev Phys. Inst.* **45** 337 (2018); *Kratk. Soobsch. Fiz. Fiz. Inst. Akad. Nauk* **45** (11) 14 (2018)
48. Lisdat Ch et al. *Phys. Rev. Research* **3** L042036 (2021) https://doi.org/10.1103/PhysRevResearch.3.L042036
49. Kolachevsky N N *Phys. Usp.* **54** 863 (2011); *Usp. Fiz. Nauk* **181** 896 (2011)
50. Vishnyakova G A et al. *Phys. Usp.* **59** 168 (2016); *Usp. Fiz. Nauk* **186** 176 (2016)
51. Golovizin A et al. *Nat. Commun.* **10** 1724 (2019)
52. Golovizin A A et al. *Nat. Commun.* **12** 5171 (2021)
53. Katori H et al. *Phys. Rev. Lett.* **91** 173005 (2003)
54. Taichenachev A V et al. *Phys. Rev. Lett.* **101** 193601 (2008)
55. Katori H et al. *Phys. Rev. Lett.* **103** 153004 (2009)
56. Fedorova E et al. *Phys. Rev. A* **102** 063114 (2020)
57. Mishin D A et al. *Quantum Electron.* **52** 505 (2022); *Kvantovaya Elektron.* **52** 505 (2022)
58. Provorchenko D et al. *Atoms* **11** (2) 30 (2023)
59. Drever R W P et al. *Appl. Phys. B* **31** 97 (1983)
60. Tsyganok V V et al. *Phys. Rev. A* **107** 023315 (2023)
61. Kramida A, Ralchenko Yu, Reader J and NIST ASD Team, NIST Atomic Spectra Database, Version 5.11, 2023. National Institute of Standards and Technology, Gaithersburg, MD. February 22, 2024; https://physics.nist.gov/asd, https://dx.doi.org/10.18434/T4W30F
62. Giglberger D, Penselin S *Z. Phys.* **199** 244 (1967) https://doi.org/10.1007/BF01326434
63. Sugar J, Meggers W F, Camus P *J. Res. Natl. Bur. Stand. A* **77** 1 (1973)
64. Tsyganok V V et al. *J. Phys. B* **51** 165001 (2018)
65. Gerlach W, Stern O *Z. Phys.* **9** 349 (1922) https://doi.org/10.1007/BF01326983
66. Virgo W L *Am. J. Phys.* **81** 936 (2013)
67. Khlebnikov V A et al. *Phys. Rev. Lett.* **123** 213402 (2019)
68. Blatt S et al. *Phys. Rev. A* **80** 052703 (2009)
69. Golovizin A et al. *JETP Lett.* **119** 659 (2024); *Pis'ma Zh. Eksp. Teor. Fiz.* **119** 645 (2024)
70. Afanasiev A E et al. *Opt. Laser Technol.* **148** 107698 (2022)
71. Liang D, Bowers J E *Light Adv. Manufacturing* **2** (1) 59 (2021)
72. Cheng H et al. *APL Photon.* **8** 116105 (2023) https://doi.org/10.1063/5.0174384
73. Vassiliev V V, Zibrov S A, Velichansky V L *Rev. Sci. Instrum.* **77** 013102 (2006) https://doi.org/10.1063/1.2162448
74. Newman Z L et al. *Optica* **6** 680 (2019)
75. Hu Y et al. *Nat. Photon.* **16** 679 (2022)